

## Supplementary Information

### High-Throughput Fabrication of Cell-Laden 3D Biomaterial Gradients

Carlos F. Guimarães<sup>1,2</sup>, Luca Gasperini<sup>1,2</sup>, Raquel S. Ribeiro<sup>1,2</sup>, Andreia F. Carvalho<sup>1,2</sup>,  
Alexandra P. Marques<sup>1,2</sup> and Rui L. Reis<sup>1,2,\*</sup>

<sup>1</sup>3B's Research Group — Research Institute on Biomaterials, Biodegradables and Biomimetics, University of Minho, Headquarters of the European Institute of Excellence on Tissue Engineering and Regenerative Medicine, Guimarães, Portugal.

<sup>2</sup>Life and Health Sciences Research Institute, 3B's Research Group on Biomaterials, Biodegradables and Biomimetics – Portuguese Government Associate Laboratory, University of Minho, Braga and Guimarães, Portugal.

\*e-mail: [rgreis@i3bs.uminho.pt](mailto:rgreis@i3bs.uminho.pt)

## **Materials and Methods**

### **Hydrogel Fabrication and Characterization**

Gellan Gum (GG) (Gelzan, Sigma-Aldrich) solutions were prepared by dissolution of the powder in water at 90°C. After dissolving, it was mixed 50:50 with a 0.5M Sucrose solution, yielding a 0.25M sucrose final solution<sup>1</sup>. Gellan Gum was crosslinked by the addition of Calcium Chloride (CaCl<sub>2</sub>) 0.1M solution. Gelatin Methacryloyl 80% DS (Sigma-Aldrich) solution was prepared in 0.25M Sucrose in water containing 0.3% 2-Hydroxy-4'-(2-hydroxyethoxy)-2-methylpropiophenone (Irgacure, Sigma-Aldrich). UV crosslinking was induced under UV light (320-500nm) (Omniculture series 2000) for 50 seconds at 0.6mW/cm<sup>2</sup> at a distance of 8 cm from the lamp. GG/GelMA Blends were fabricated by mixing both solutions and combining both crosslinking (first ionic for a quick stabilization of the structure and then UV for crosslinking the GelMA component). GelMA and GG up to 0.5% were sterilized by filtration. The 0.5% solution was filtered, freeze dried under sterile conditions, and the obtained powder was used to prepare the 1% GG solution.

The characterization of precursor solutions and hydrogels was performed on a Rheometer (Malvern Kinexus Pro+). For the derivation of storage and loss moduli, hydrogels were first subjected to a strain amplitude sweep in order to find the linear elastic region, which was then used for a frequency sweep and moduli derivation. Stress relaxation tests were performed by applying a 10% shear strain and following the change in shear stress ( $G(t)$ ) over time, normalized against the initial  $G(0)$ .

### **Adipose stromal Cell Isolation and Encapsulation**

Human adipose-derived stromal/stem cells (hASCs) were isolated as previously described<sup>2</sup>. Briefly, cells were obtained from lipoaspiration surgeries of healthy individuals, after consent and under a collaboration agreement between Hospital da Prelada (Porto) and 3B's Research Group, approved by the respective ethical committees. The adipose tissue samples were subjected to enzymatic digestion (0.05% collagenase type II (Sigma-Aldrich) under agitation for 45 min at 37 °C), and after centrifugation and red cell lysis, hASCs were selected by plastic adherence. Cultured ASCs are characterized as CD73<sup>+</sup>/CD90<sup>+</sup>/CD105<sup>+</sup>/CD44<sup>+</sup>/CD45<sup>-</sup>/CD31<sup>-</sup> cells<sup>2,3</sup>.

hASCs were expanded and cultured in alpha-MEM (Gibco) with 10% FBS (Gibco) and 1% antibiotic, antimycotic (Gibco) up to passage 4. Suspensions of 1M cells /ml and 3M cells /ml were used in the fabrication of GG fibres and gradients, and in the uniform GG/GelMA fibres, respectively. Prior to encapsulation, hASCs were detached with TrypLE Express (Gibco), washed, counted to reach proper numbers according to the desired concentration, and were then resuspended directly in the hydrogel precursor solutions before gelation. For the differentiation studies, the cell-laden fibres were cultured as indicated in the StemPro Chondrogenesis Differentiation Kit Medium (Gibco) for triggering of chondrogenic differentiation, and in alpha-MEM supplemented with 10% FBS, 1% ATB, 34 µM of D-pantothenate (Sigma-Aldrich) and 66 µM of biotin (Sigma-Aldrich), 200 nM of insulin (Sigma-Aldrich), 1 µM of dexamethasone (Sigma-Aldrich), 250 µM of 3-isobutyl-1-methylxanthine (IBMX) (Sigma-Aldrich), and 5 µM of troglitazone (Sigma-Aldrich) for the adipogenic differentiation. Throughout the work, hASCs from 4 different donors were used at random.

### **Microfluidic Setup and Gradient Fabrication**

A custom microfluidic system was employed to obtain the different gradients<sup>4</sup>. An OB1 pressure controller and flow sensors (Elvesys) were used to regulate the flow of

different hydrogel's precursor solutions. Gradient fabrication started with a first endpoint material flow, which was linearly reduced according to a ramp-like function, while the second endpoint material gradually increased in the reverse manner (**fig 1B**). The flows were forced through a custom-built T-junction chip with two herringbone mixing stages (Translume) to ensure the disruption of purely laminar flow and lead to precursor mixing and therefore uniform blending of the two endpoint materials. The flowing blend was then directed into a linear microfluidic chip (Dolomite) and wet-spun into a 0.1M CaCl<sub>2</sub> (Sigma-Aldrich) solution to crosslink the GG. In the case of GG/GelMA gradients, UV light was further applied to the gradient fibre for 10 seconds upon collection. In all experiments, both endpoint materials were stained with soluble microfluidic dyes (Elvesys) in order to track the gradient formation in real-time. A third, transparent material (0.5% Gellan Gum) was used to separate the different gradients, visibly showing the ending of one and beginning of another (**SVideo**). This allowed a clear visualization of the gradient start and end thus facilitating gradient collection. A looping algorithm was employed in the controller software in order to fabricate a gradient, push the intercalating solution, create a new gradient, and so forth, sequentially producing as many gradients as loop turns inputted. Each cell-laden gradient was collected and placed in 6-well cell culture plates (Sigma, TPP) under the conditions of culture described above.

### **Gradient Tracking**

To track the composition of the gradients and to validate their gradually changing components, three methods were used throughout this work:

The first one, previously described, consisted on the dissolution of soluble microfluidic dyes (Elvesys) of different colours which allowed tracking the gradient formation in real time (Supplementary Video).

Since these dyes diffuse, a more robust method was needed to confirm the gradient formation and material transition. For this purpose, we blended the endpoint materials (GG 1% and GG 0.5%) with either green FITC-GG (Yielding the GG 1% (FITC) nomenclature of the main text) or red RITC-Hyaluronate (1.5MDa, Lifecore) (Yielding the GG 0.5% (RITC) nomenclature), at 1:100 volume ratio. The fluorescent GG crosslinks together with the normal GG and the Hyaluronate, having high molecular weight, remains trapped in the crosslinking GG, allowing the observation of the gradient long after fabrication without the concern of diffusion. To observe the gradient distribution, the full gradients with fluorescent trackers were imaged and the contribution of each fluorescent tracker was measured along X-axis using ImageJ. An additional method was employed to observe the gradient formation, in the GG-GelMA gradients. Being composed of highly different molecules, the gradient was fabricated as previously reported without any dye and later stained with the ColF probe (Immunochemistry Technologies) according to the manufacturer's instructions. The specificity of ColF to collagen and its denaturated forms<sup>5</sup> was then used to image and observe the presence of the gradient by targeting the Gelatin component.

### **Cellular Viability and Immunocytochemistry**

Cellular Viability was tracked by incubating cell-laden hydrogels and fibres with Calcein AM 1:1000 (Molecular Probes) and Propidium Iodide 1ug/ml (Molecular Probes) for 30 minutes, followed by 2 washes in PBS before imaging.

For immunocytochemistry, samples were fixed in formalin 10% for 10 mins at room temperature (RT), washed with PBS and incubated with 0.2% Triton X-100 (Thermo Fisher) in PBS for 12 minutes to enhance cell membrane permeability. After washing, non-specific interactions were blocked by incubation with 3% BSA (Sigma-Aldrich) in PBS for 30 minutes. Afterwards, samples were incubated with the primary antibody in

1% BSA for 2 hours at RT, washed with PBS and incubated with the secondary antibody for 1 hour at RT. Cell cytoskeleton and nuclei were also stained with Phalloidin-TRITC (Sigma-Aldrich) 2ug/mL and DAPI (Biotium) 4ug/mL simultaneously added with the secondary antibody. At the end, samples were washed with PBS and imaged or kept in PBS at 4°C, in the dark until that.

Primary antibodies used: Rabbit Anti-SOX9 1:500 (Merck), Rabbit Anti-PPAR-gamma 1:100 (Abcam), Rabbit Anti-Ki67 1:250 (Abcam), Mouse Anti-YAP 1:50 (Santa Cruz), Rabbit Anti-Paxillin 1:250 (Abcam).

Secondary Antibodies used: Alexa 594 donkey-anti-mouse 1:500 (Molecular Probes), Alexa 488 donkey anti-rabbit 1:500 (Molecular Probes).

### **Microscopy and Image Analysis**

Whole fibre and gradients were imaged using an Axio Observer Inverted Microscope (Zeiss), with an automated stage allowing for tile scan acquisition. Low-magnification was used together with Z-stacking for image acquisition. Z-stacks images of the fibres and gradients were processed to obtain maximum projection extended depth of focus. This allowed for a good balance between fast imaging (under 20 minutes per full gradient) and translation of responses from 3D to 2D, maximizing throughput and overcoming 3D computational limitations<sup>6</sup>. Additionally, higher resolution images of specific fibre details were acquired in higher magnification or in an Inverted Confocal Laser Scanning Microscope (Leica).

Images taken for cell screening were then analysed with the CellProfiler software<sup>7</sup>. Generally, gradients were imaged as a whole whereas macro hydrogels were imaged at random positions on 3 sections per replicate. In all cases, a minimum of 100 cells was considered for quantification. Specific pipelines were used to process cell markers as

objects (Fig. S6) and from there derive count numbers, SOX9/Phalloidin and PPAR- $\gamma$ /Phalloidin total pixel ratios (Mander's Co-localization Coefficient) and intensity of the distinct signals. The Marker/Phalloidin pixel ratios are in practice a direct normalization of the projected marker area to the projected cell area, reducing variability effects. Cell responses on gradients were tracked with object X position and plotted as a function of location along the gradient. Throughout the document, individual graphs of gradient responses represent a single replicate since the position of each cell is never the same between replicates.

Additionally, in order to identify trends within the gradients, cell responses were tested for positive or negative correlations, as described in the statistical section.

### **Western Blot**

For protein extraction, cell-laden hydrogels were collected from culture and washed thoroughly with cold PBS. Afterwards, hydrogels were transferred to an Eppendorf containing radio-immunoprecipitation assay (RIPA) buffer supplemented with 1:200 protease inhibitor (Sigma-Aldrich). Using a pestle, hydrogels were macerated until a slurry mixture was obtained. Samples were then centrifuged at 13000 rpm, 4°C for 15 minutes. The supernatant (protein extract) was collected and stored at -80°C until quantification.

Protein Quantification was performed using the Pierce BCA kit (Thermo Fisher), according to manufacturer's instructions. 10ug of protein were mixed with gel loading buffer composed of tris-HCL (ph8.8) (Sigma-Aldrich), 0.05% Bromophenol Blue (Sigma-Aldrich), 6% SDS (NZYtech), 30% Glycerol (Honeywell), 10% EDTA NaOH (6mM) (Lonza) and Dithithreitol (DTT) (Sigma-Aldrich), heated for 60°C 10 minutes, 90°C 5 minutes for denaturation, and then loaded into 10% SDS Polyacrylamide gels (Sigma-Aldrich), together with a molecular weight marker (Thermo Fisher). After

electrophoresis, bands were then transferred to a nitrocellulose membrane (GE Healthcare) and incubated with Ponceau Solution (Sigma-Aldrich). After washing excess ponceau, the blots were blocked in 5% Skim Milk in Tris-Buffered Saline (TBS) for 1h. After blocking, membranes were incubated with the primary antibody prepared in 5% Skim Milk in TBS overnight at 4°C. After thorough washing, the bound antibody was detected by incubation with an alkaline phosphatase-linked secondary antibody (Sigma-Aldrich) diluted in 5% skim milk TBS for 1h at RT. After washing, bands were observed using an AP conjugate Substrate kit (Biorad), followed by scanning on an EPSON V600 Scanner. Band intensities were quantified through the FIJI (ImageJ) software.

Primary antibodies used: Rabbit Anti-SOX9 1:500 (Merck), Rabbit Anti-Paxillin 1:3000 (Abcam), Mouse Anti-YAP 1:100 (Santa Cruz), Rabbit Anti-Tubulin (Abcam) (loading Control) 1:500.

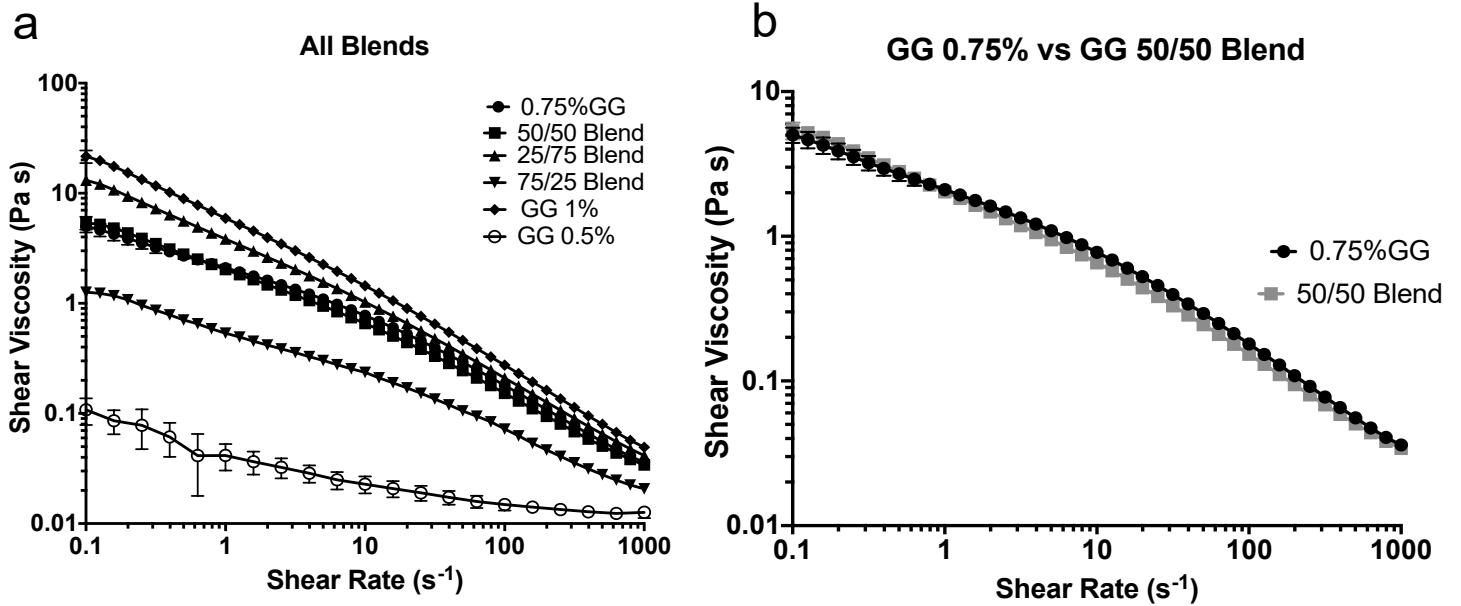
Secondary antibodies used: Goat-Anti-Rabbit AP-Conjugated 1:3000 (Sigma-Aldrich), Horse-Anti-Mouse AP-Conjugated 1:3000 (Vector Laboratories).

### **Statistical Analysis**

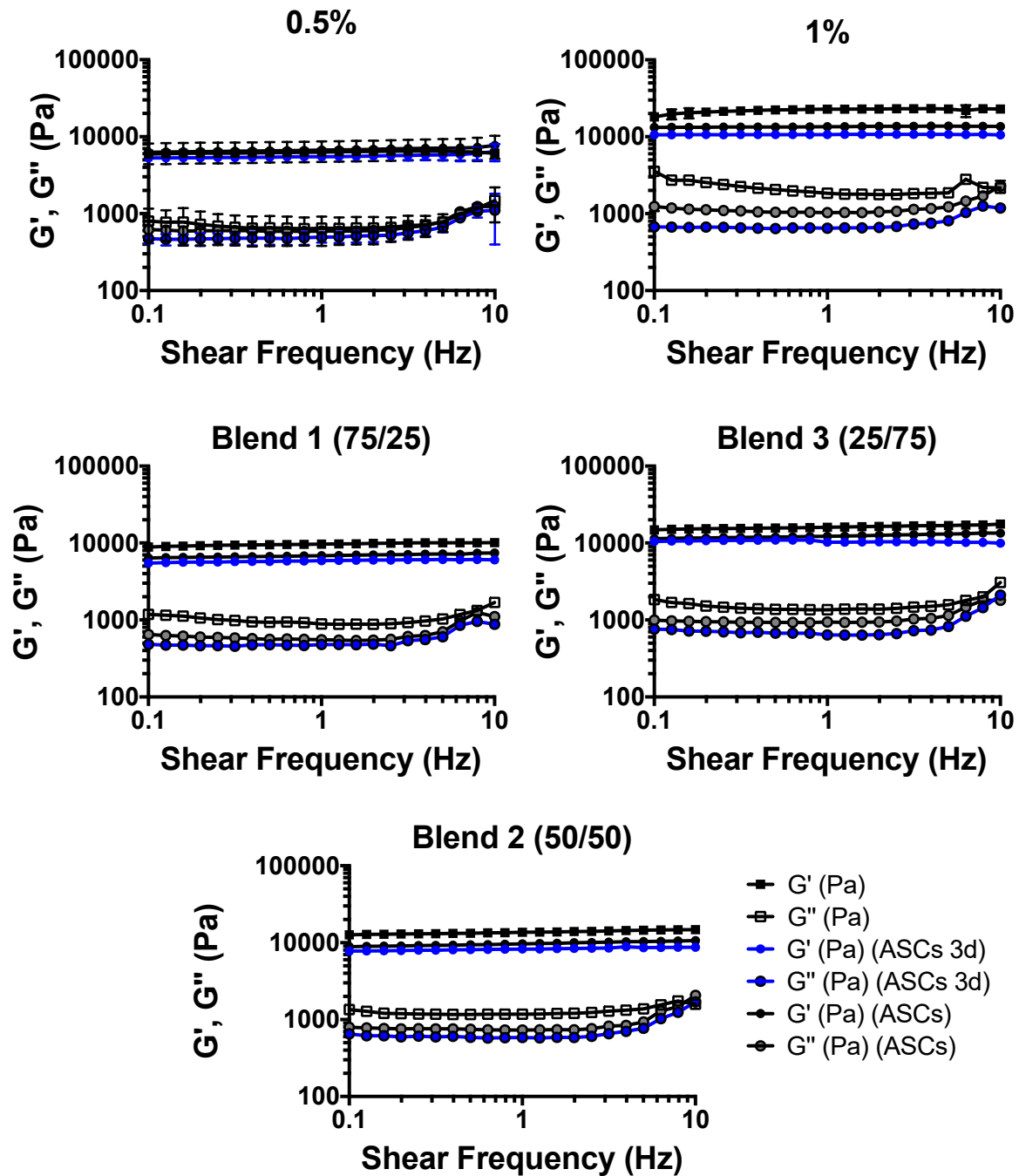
Statistical Analysis was performed through the Prism Software (Graphpad, v6).

Generally, the sets of samples were initially tested for Gaussian distribution. In case of a positive result, samples were analysed by Ordinary 1-way ANOVA followed by Dunnett's Multiple Comparison Test. In the case of negative normality result, Kruskal-Wallis test followed by Dunn's Multiple Comparison Test was used instead. In the case of gradient responses, upon negative Gaussian distribution, nonparametric Spearman correlation values were computed. For all gradients, only data sets with more than 100 cell events were considered for analysis. In all cases, differences/correlations were considered statistically significant when  $p < 0.05$ .

## Supplementary Figures:

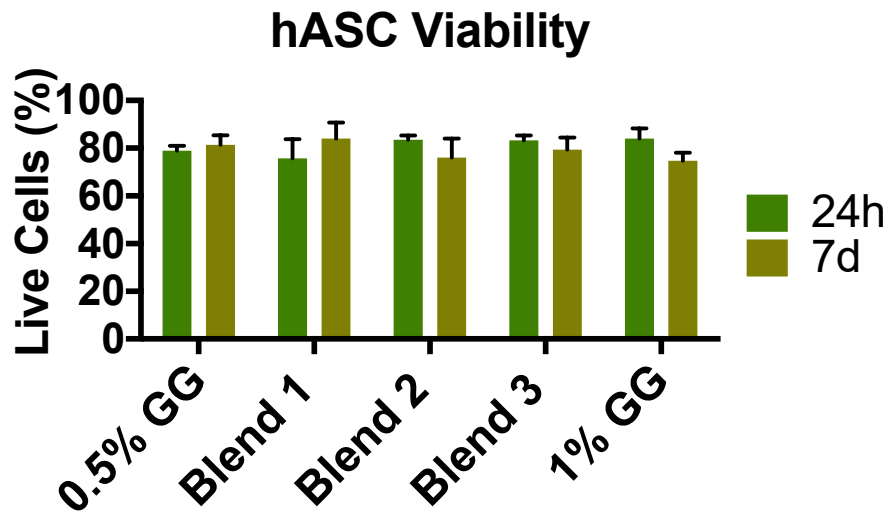
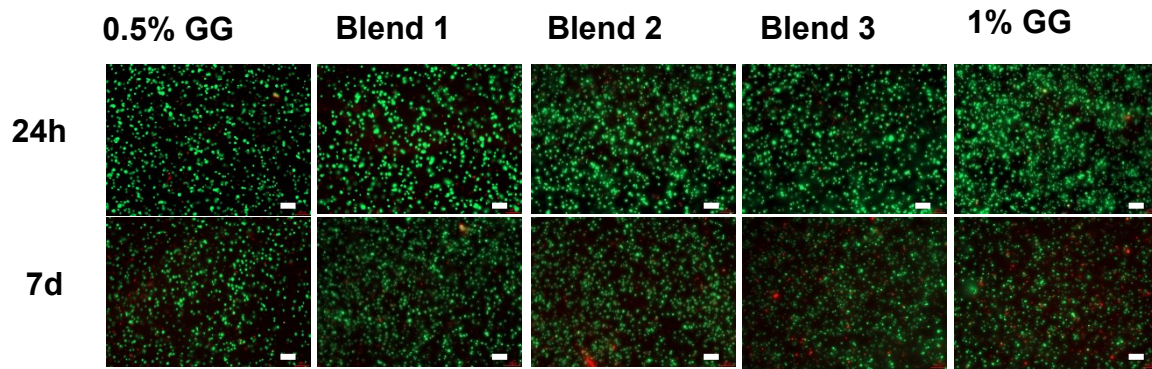


**S1 – Gellan Gum Rheology** – Analysis of the Shear viscosity of the different blends of Gellan Gum (a), showing the increase in viscosity with increasing polymer concentrations. The comparison of a 0.75% GG with a 50/50 blend of GG 0.5% and GG 1% (b) reveals that formulating the material at an intermediate concentration or obtaining it by mixing from different concentrations yields a similar mixture. The blending method was therefore followed once it mimics what happens in the microfluidic mixing, knowing it is the same as dissolving the polymer to the equivalent concentration. N=3.

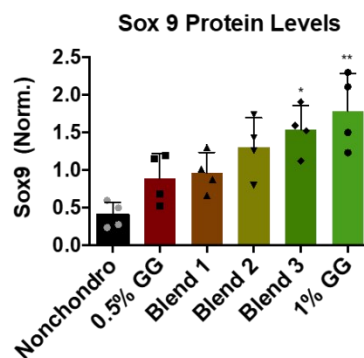
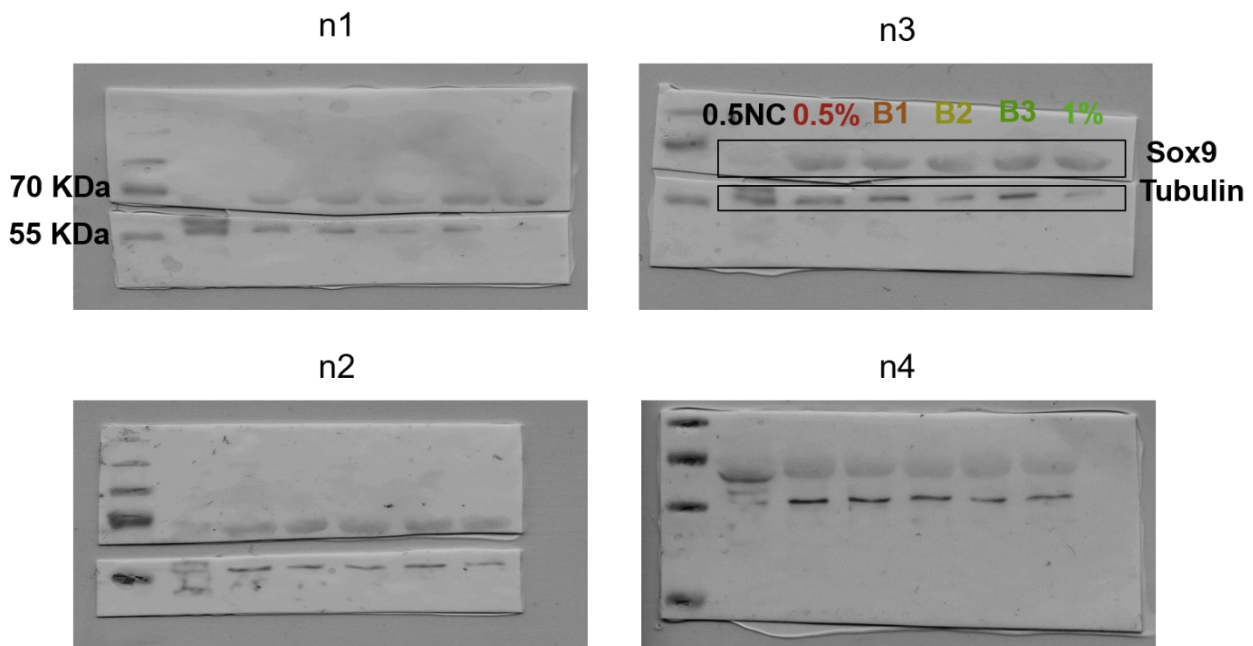


**S2 – Gellan Gum Hydrogel Oscillation** – All hydrogels were tested within their linear elastic region, performing a shear frequency sweep to derive the  $G'$  and  $G''$  of the pure hydrogel, upon ASC encapsulation (ASCs) and after encapsulation and 3 days of culture (ASCs 3d). There is a slight decrease in mechanics on the stiffer gels upon ASC encapsulation, which is in most cases not further affected by short term cell culture.

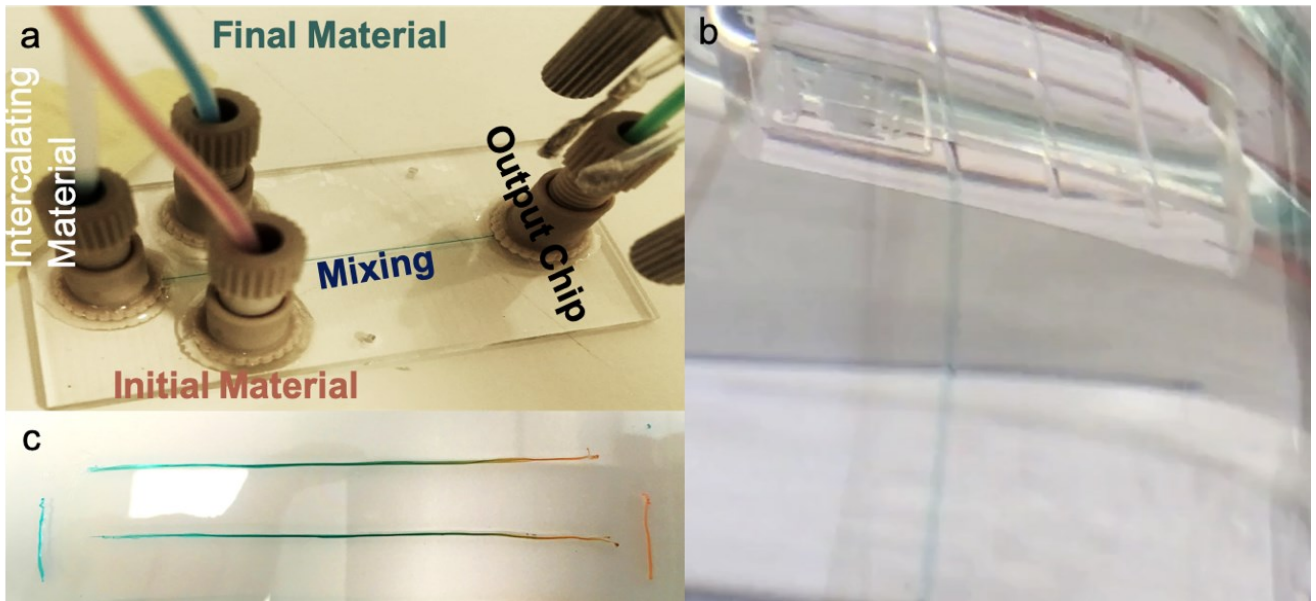
N=5.



**S3: Encapsulated hASC Viability:** Human adipose-derived stromal/stem cells (hASCs) viability (live Calcein AM (Green) and dead Propidium Iodide (Red) cells) remained high shortly after encapsulation and upon 1 week of culture (scale bar 100 $\mu$ m). Image analysis after Calcein AM staining shortly after encapsulation revealed decreasing projected cell areas in the higher concentration hydrogels as reported in the maintext.

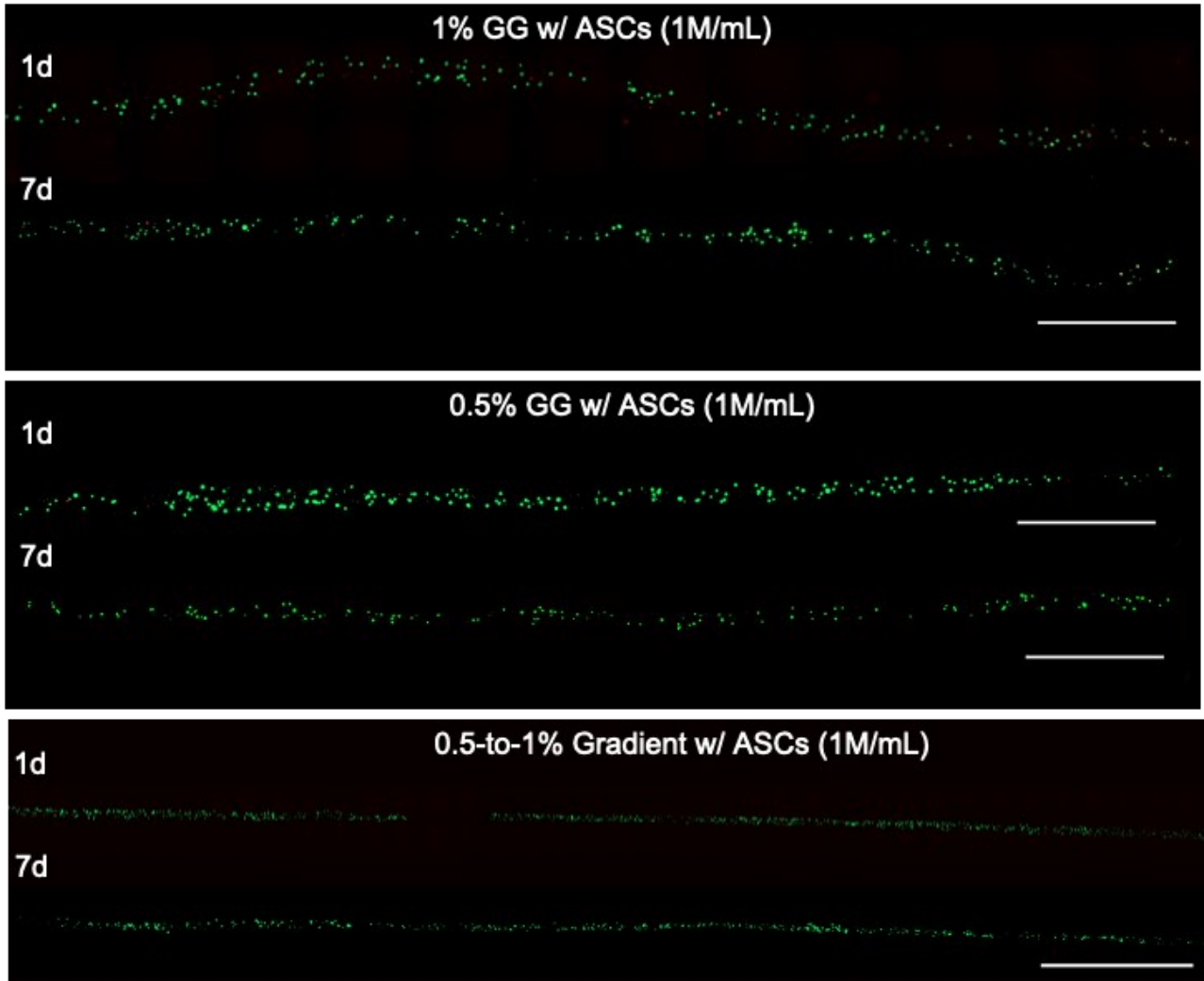


**S4- Sox9 Western Blot** – Western blots for validation of Sox9 screening in the different hydrogels upon 1 week of chondrogenic culture. Different pictures represent replicated experiments. On the bottom, the semi-quantification of SOX9 protein was performed, confirming the image screening results. Statistical values: \*p<0.05, \*\*p<0.01, \*\*\* p<0.001, compared to control (Nonchondro, meaning no chondrogenic stimuli. NC – Non-chondro, B1 – Blend 1, B2 – Blend 2, B3 – Blend 3. Blend compositions are detailed in the main text.

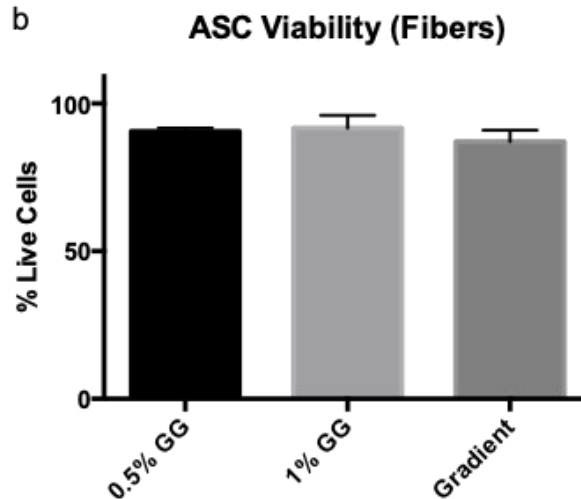


**S5 – Gradient Fabrication** – The different endpoint materials (stained red and blue) are pushed to flow into a T-junction mixer chip (a), which disrupts the laminar flow allowing for an axially-uniform fiber instead of a Janus-like structure. This is in turn connected to a linear output chip that releases the solution into a crosslinking bath (b). The gradients are sequentially produced and collected; their composition tracked in real time by soluble food-dye staining – macroscopic view of 2 gradients immediately after production comparing to 2 single-material segments (c).

a

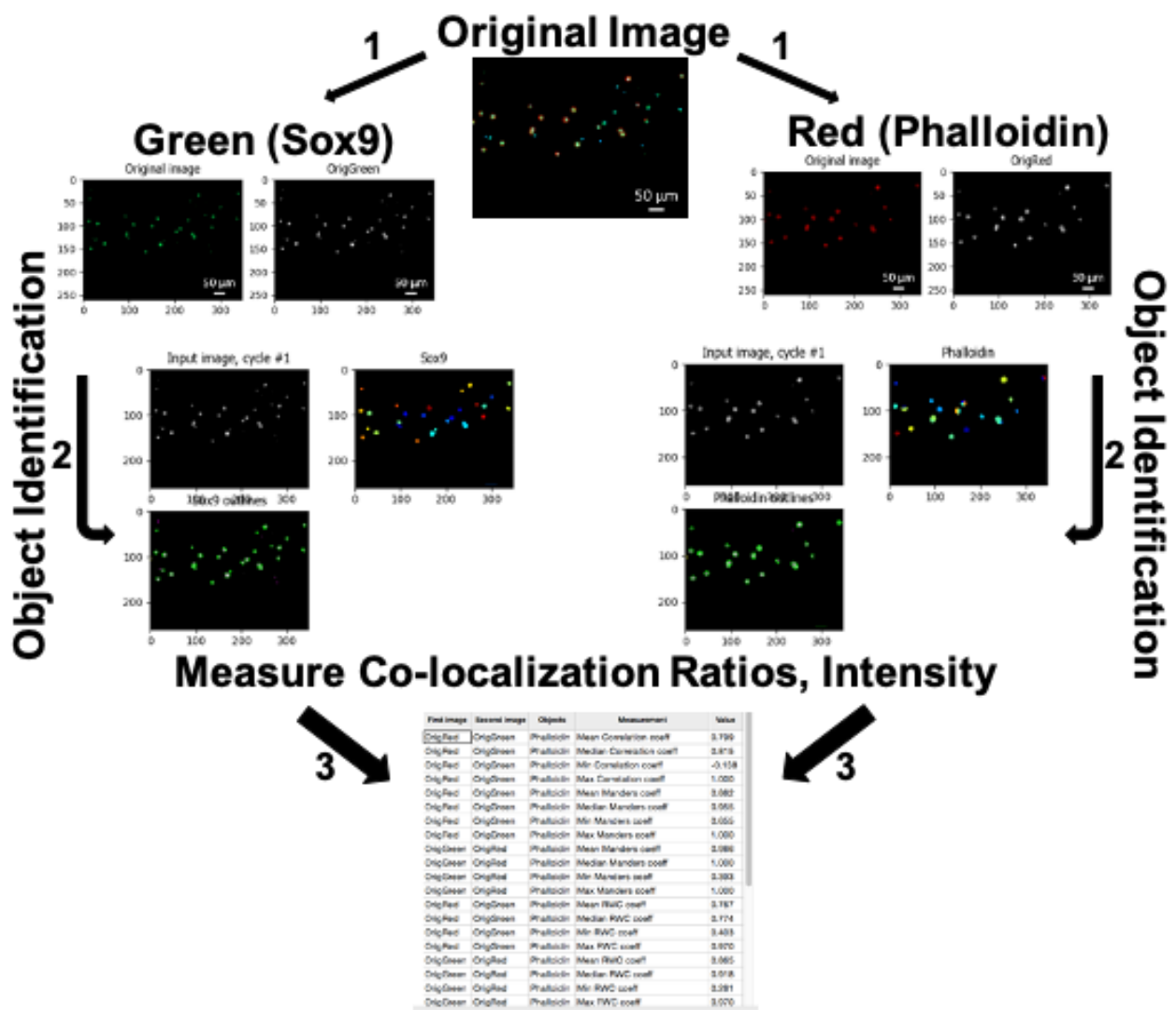


b



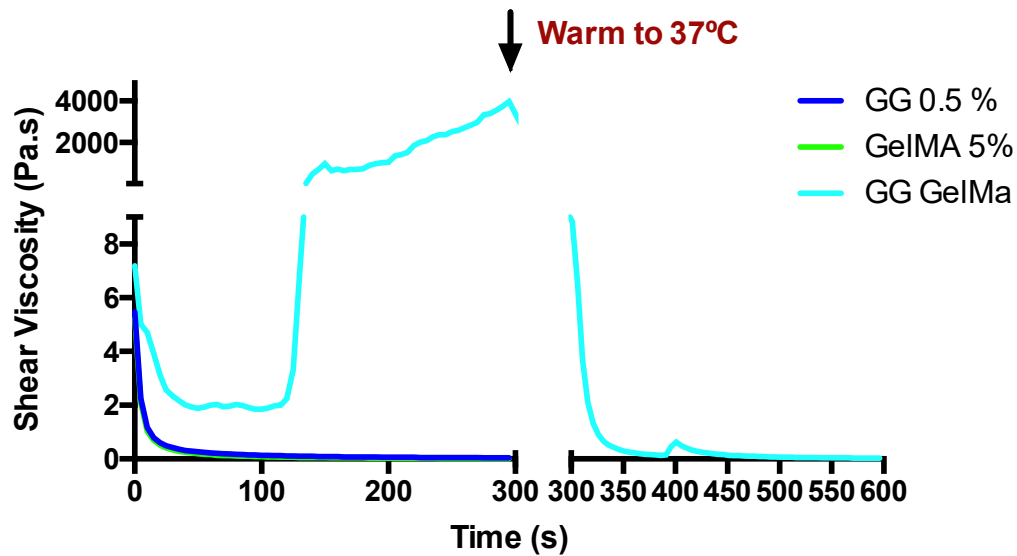
**S6 – ASC Viability Assessment** – ASC viability in uniform fibers and gradients is not impacted negatively by microfluidic manipulation, with most cells remaining viable (a, calcein AM signal in green, propidium iodide signal in red, scale bar 5mm). The

percentage of viable cells is of 80% or higher in all cases (b), being similar to or higher than that of discrete hydrogels due to thinner structure and faster nutrient/waste diffusion from the fibers. N=3.



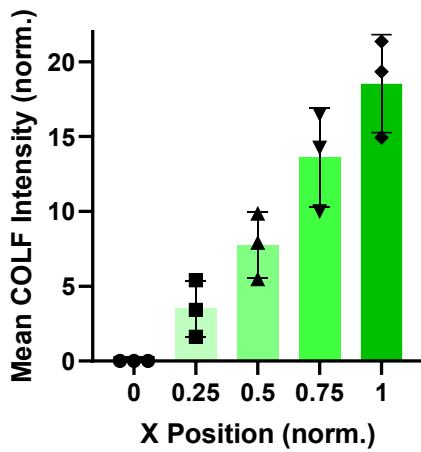
**S7 – Image Analysis Pipeline Example** – The original image is processed and separated according to the different channels (1). In this example, green is selected for Sox9 and Red for Phalloidin. Cell-profiler identifies the individual objects above a threshold of size for discarding debris/artifacts in both cases (2) and then superimposes the objects calculating co-localization values (3) as well as intensities for other approaches. Mander’s Co-localization coefficient is selected yielding the ratio of Sox9 positive pixels within the Phalloidin area, on average (uniform gels) and per-object (gradients).

## Sample Viscosity

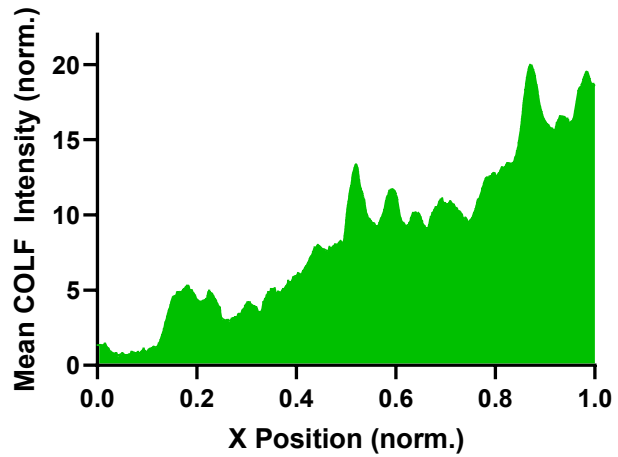


**S8 – GG/GelMA Viscosity Tests** – In order to test flow conditions for GG/GelMA gradient fabrications, the viscosity vs time of the distinct materials was assessed after mixing GelMA (37°C) and GG (25°) . At Room temperature, GG and GelMA do not see their viscosity increased for up to 5 minutes. However, when mixed, there is a fast increase in viscosity at around 120 seconds (2 minutes), suggesting thermal gelation (GelMA-induced and reversible). To prevent this from happening within the microfluidic channels, the temperature at which the materials were maintained during fabrication was kept at 37°C: When applied to the GG/GelMA mix, this temperature immediately reverses the viscosity to that of the other liquids.

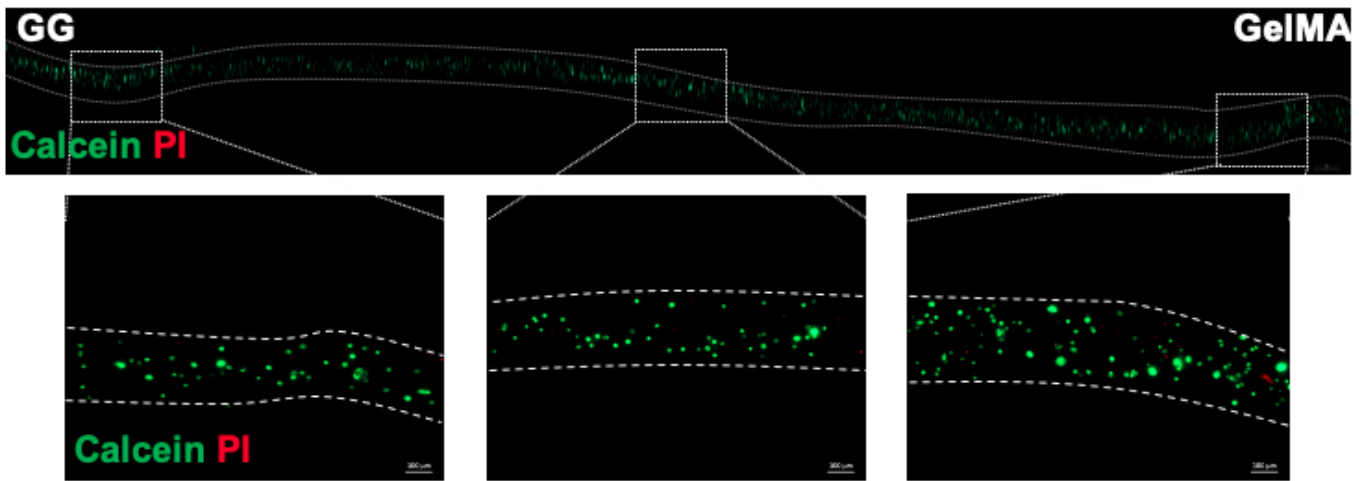
**Discrete Gelatin Level Analysis**



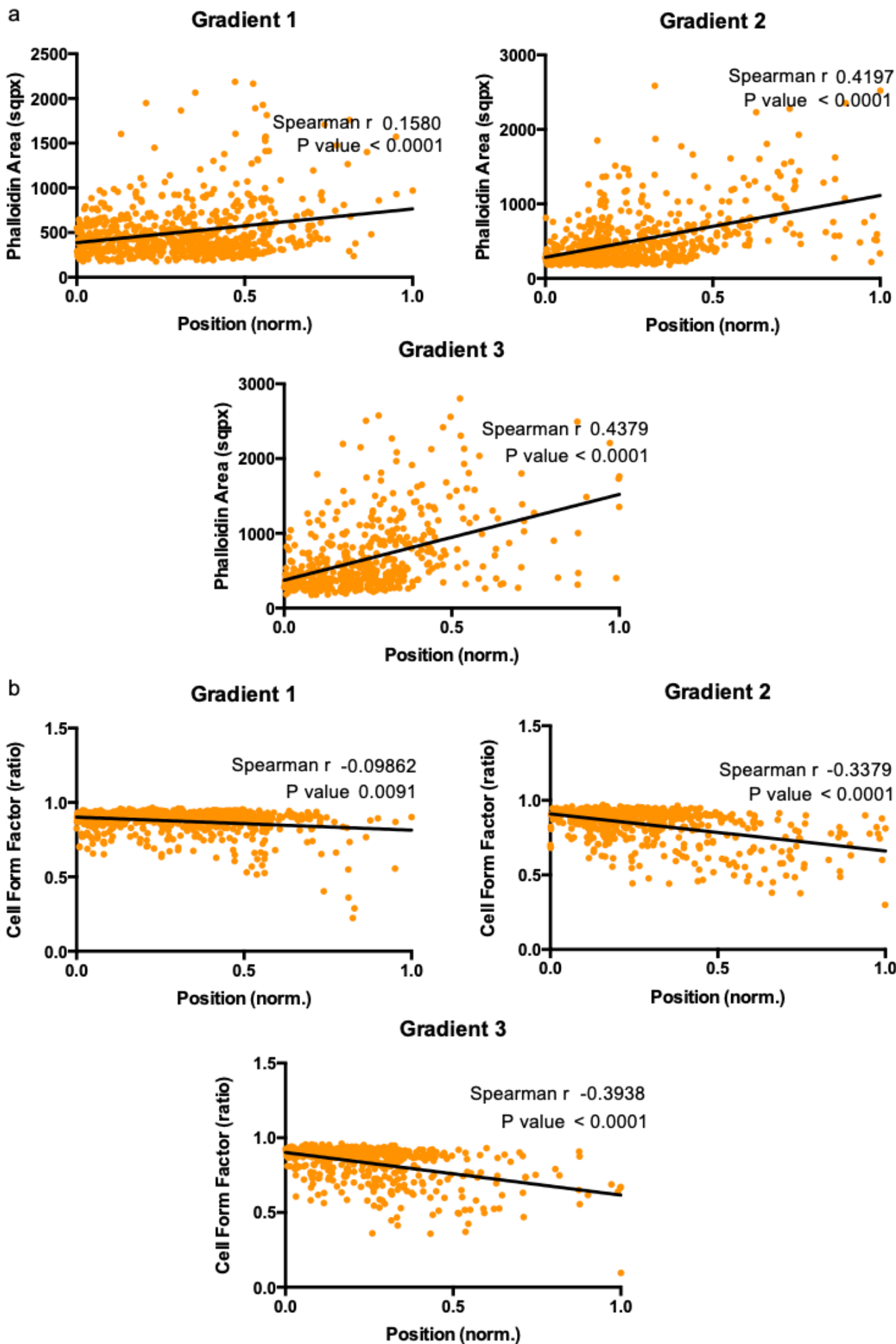
**Continuous Gelatin Level Analysis**



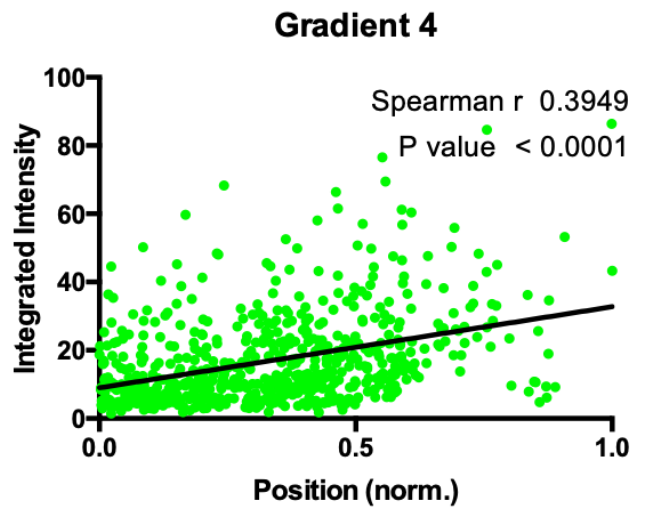
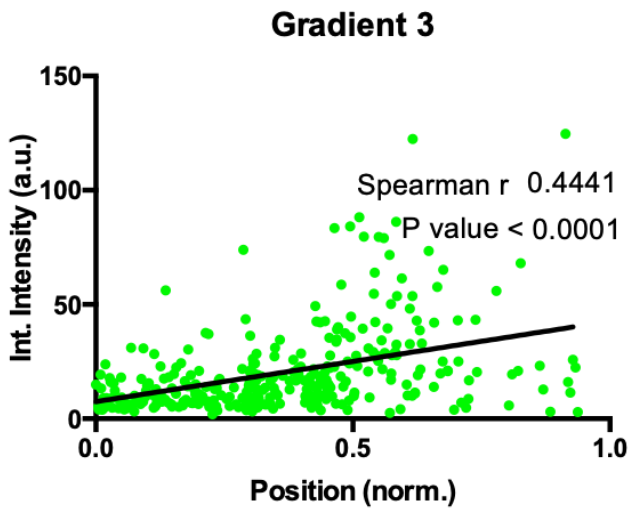
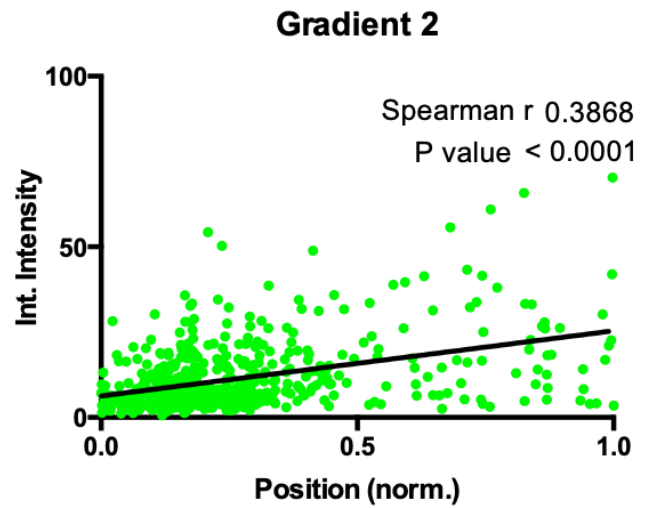
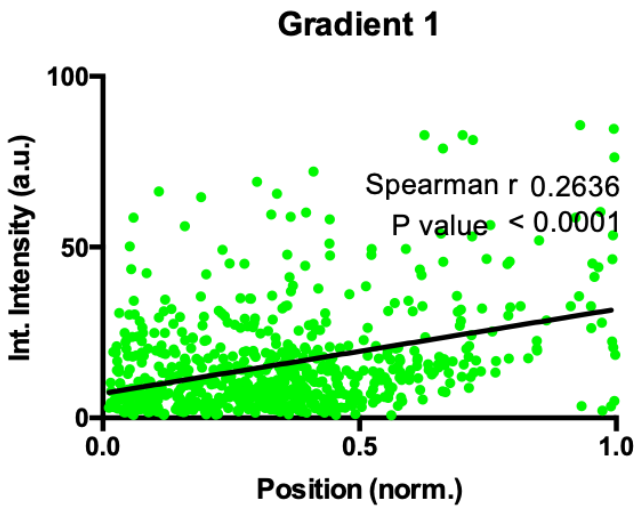
**S9 – GG/GelMA Gradients Quantification:** Quantitative analysis of the COLF signal (Gelatin staining) in 5 distinct positions of independent gradients (left) and continuous profile of the signal along the gradient (right). Both evidence a linear-like increase in the level of GelMA, agreeing with the programmed flows as well as the GG-based gradients.



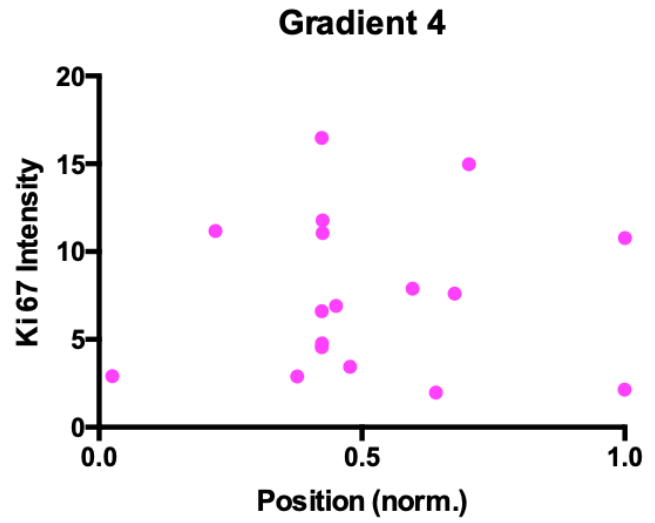
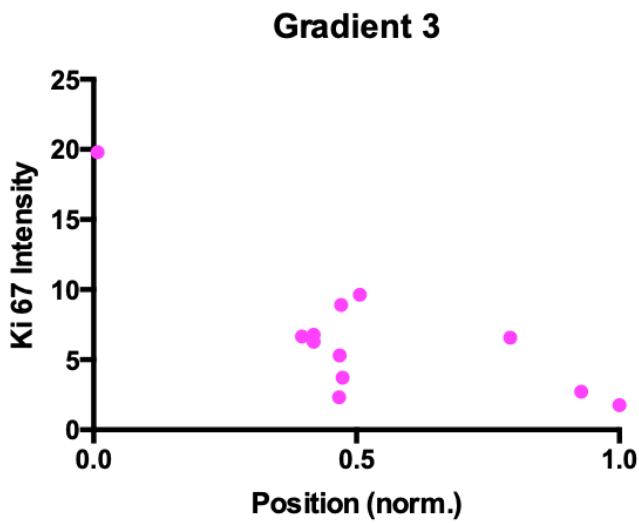
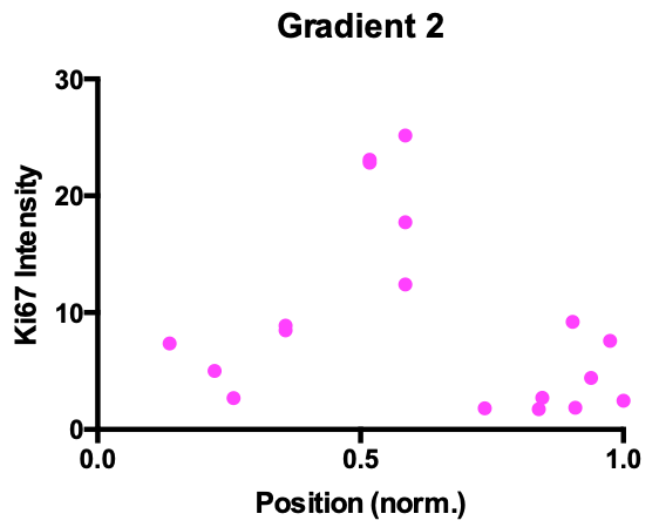
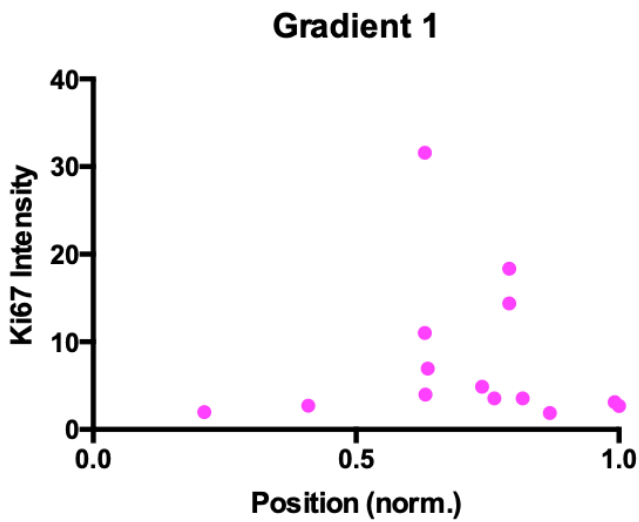
**S10 – GG/GelMA ASC Live/Dead Assay – Viability test on the GG/GelMA gradient** and some zoomed-in pictures of the beginning, middle and end. Detailed cell-by-cell plotting is present in the main text. In both cases, no significant changes are observed in the Calcein/PI proportions regardless of the material and crosslinking type.



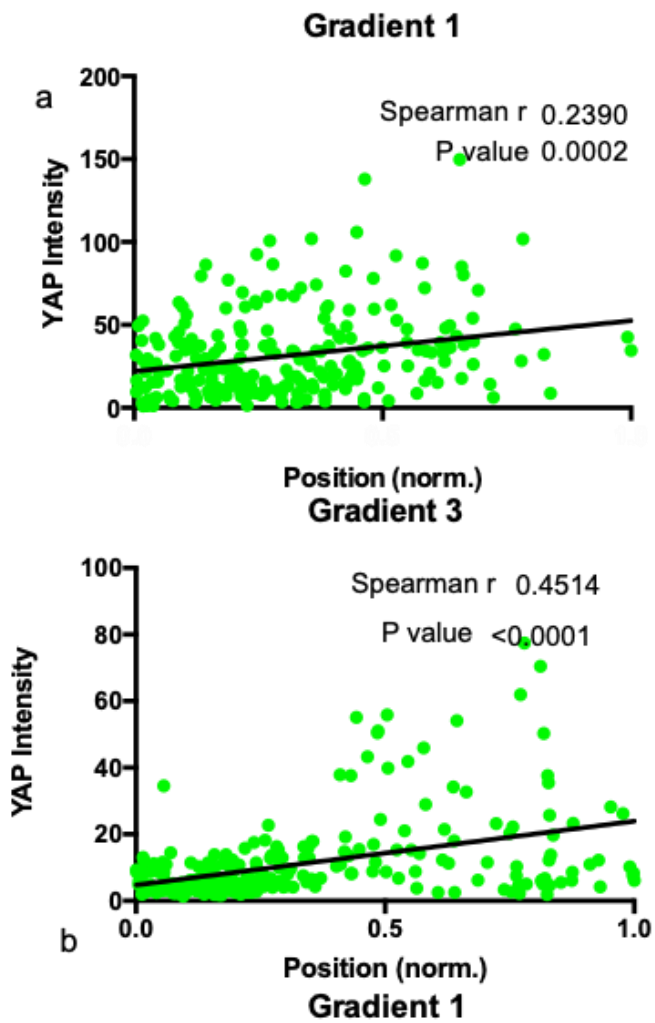
**S11 Gradients Morphology** – Analysis of cell morphology in the different gradient replicates. In all cases, significant increases in cell area (a) and decreases in form factor (b) can be observed, as well as a visible shift in area around the half position of the gradient (0.5, 1:1 GG/GelMA ratios).



**S12 Gradients Paxillin** – Analysis of paxillin responses of cells on the different gradient replicates. In all cases, a significant increase in paxillin intensity is observed as function of gradient position, hinting at increased adhesion responses from cell-GelMA interactions, as well as a visible shift in area around the half position of the gradient (0.5, 1:1 GG/GelMA ratios).

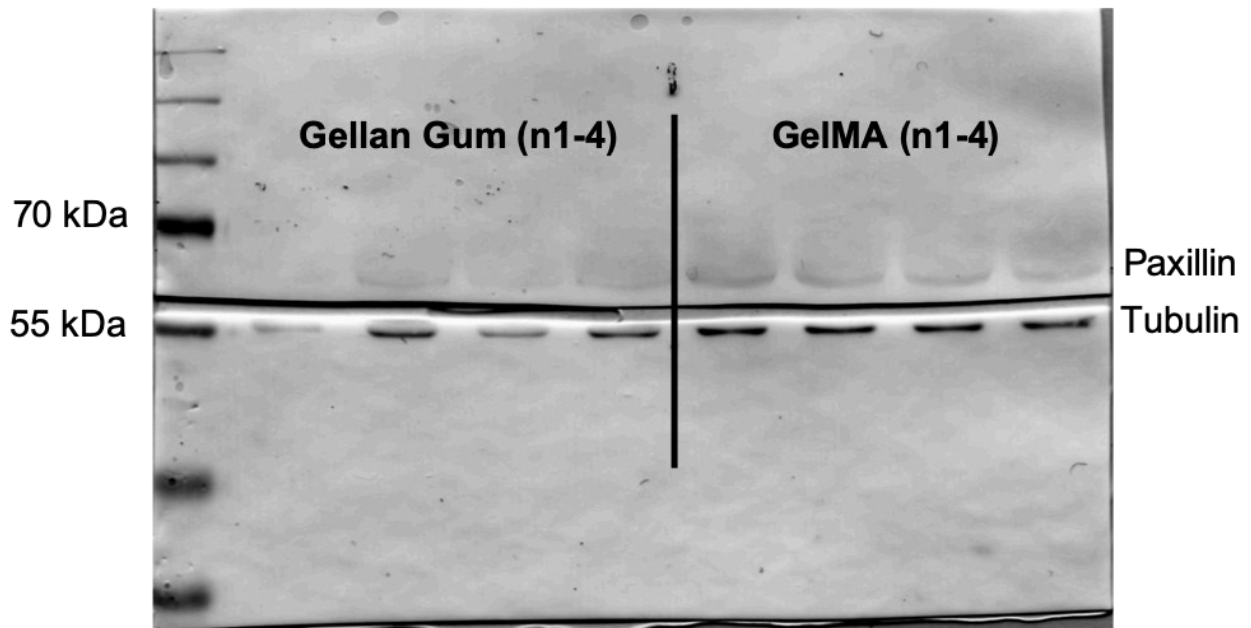


**S13 Gradients Ki-67** – Analysis of Ki-67 responses on the distinct gradient replicates. In all Cases, most Ki-67+ events appear only from half of the gradient onward, where the environment is prone to remodeling and degradation allowing cells to enter proliferation.

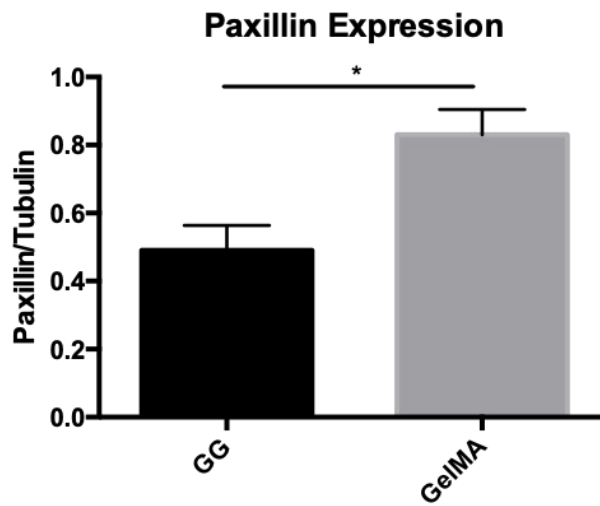


**S14 Gradients YAP** – Analysis of YAP responses. YAP intensities increase along the gradient replicates (a) but no change in the nuclear/cytoplasmic ratios was detected in any case (b).

a

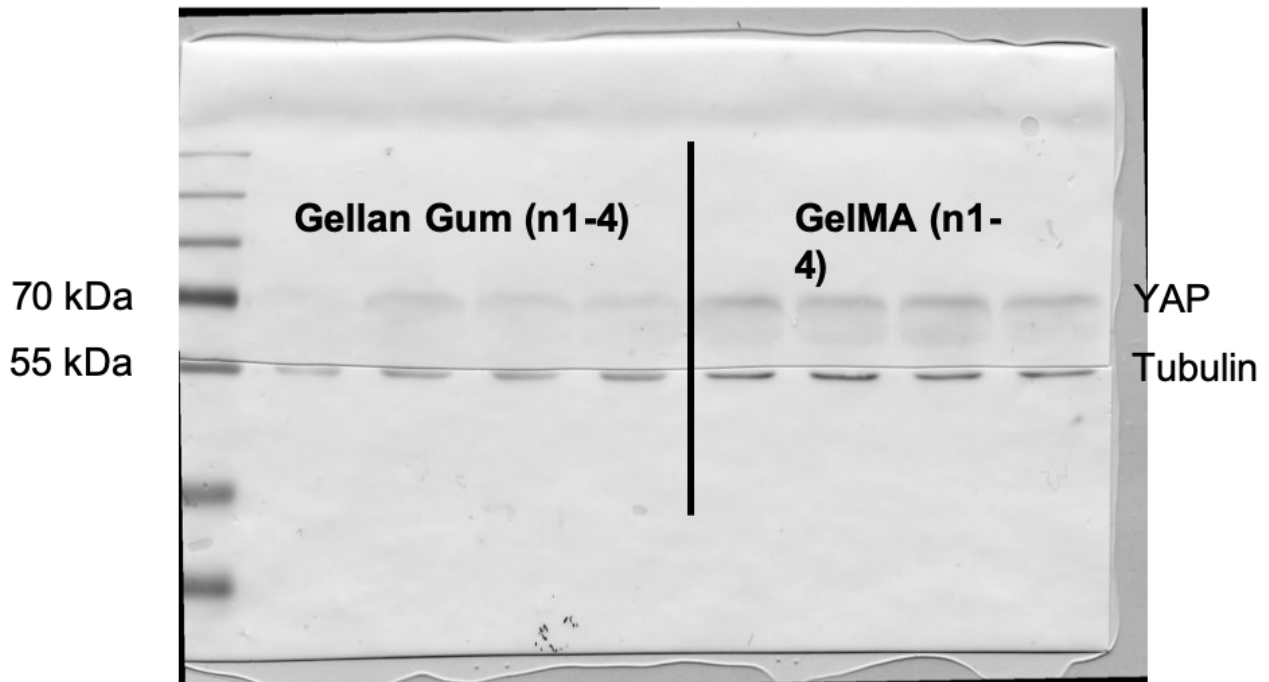


b

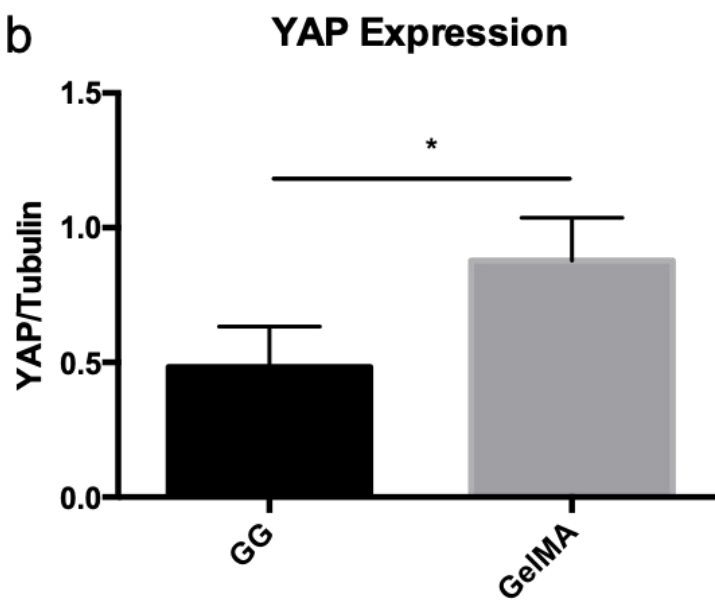


**S15 Western Paxillin** – Molecular validation of Paxillin responses on pure endpoint GG and GelMA macro hydrogels. 4 replicates of each condition were tested (a), evidencing a significant increase in paxillin expression at the molecular level (b) which validates the trends observed on the image analysis of gradients.

a



b



**S16 – Western YAP** - Molecular validation of YAP responses on pure endpoint GG and GelMA macro hydrogels. 4 replicates of each condition were tested (a), evidencing a significant increase in YAP expression at the molecular level (b) which validates the trend derived from the image analysis of the gradients.

## Supplementary Refernces:

- 1 A. F. Carvalho, L. Gasperini, R. S. Ribeiro, A. P. Marques and R. I. Reis, *J. Tissue Eng. Regen. Med.*, 2018, **12**, e1063–e1067.
- 2 M. T. Cerqueira, R. P. Pirraco, T. C. Santos, D. B. Rodrigues, A. M. Frias, A. R. Martins, R. L. Reis and A. P. Marques, *Biomacromolecules*, 2013, **14**, 3997–4008.
- 3 P. C. Baer, *World J. Stem Cells*, 2014, **6**, 256.
- 4 L. Gasperini, A. P. Marques and R. L. Reis, *WO2018078562A1*.
- 5 E. Biela, J. Galas, B. Lee, G. L. Johnson, Z. Darzynkiewicz and J. W. Dobrucki, *Cytom. Part A*, 2013, **83 A**, 533–539.
- 6 T. H. Booiij, L. S. Price and E. H. J. Danen, *SLAS Discov.*, 2019, **24**, 615–627.
- 7 L. Kamentsky, T. R. Jones, A. Fraser, M. A. Bray, D. J. Logan, K. L. Madden, V. Ljosa, C. Rueden, K. W. Eliceiri and A. E. Carpenter, *Bioinformatics*, 2011, **27**, 1179–1180.